RZ 3873 (#Z1111-003) 11/10/2011
Physical Sciences 14 pages

Research Report

Imaging the charge distribution within a single molecule

Fabian Mohn, Leo Gross, Nikolaj Moll, and Gerhard Meyer

IBM Research - Zurich, 8803 Rüschlikon, Switzerland

This is the author's version of the work. The definitive version was published in *Nature Nanotechnology*, vol. 7, no. 4, pp. 227–231 (2012) (doi:10.1038/nnano.2012.20; published online: 26 February 2012) and can be accessed here:
http://www.nature.com/nnano/journal/v7/n4/full/nnano.2012.20.html

Imaging the charge distribution within a single molecule

Fabian Mohn,* Leo Gross, Nikolaj Moll, and Gerhard Meyer

IBM Research – Zurich, 8803 Rüschlikon, Switzerland

(Dated: November 10, 2011)

Abstract

Knowing the charge distribution within individual nanostructures or molecules on surfaces is important for applications in which charge is to be moved on the nanometre scale, such as nanoelectronics and organic photovoltaics. Scanning tunneling microscopy (STM) and atomic force microscopy (AFM) are established tools for studying electronic and structural properties of surfaces and adsorbates with atomic precision [1–7]. However, the charge distribution is not directly accessible with these techniques. Kelvin probe force microscopy (KPFM), on the other hand, can be used to measure the local contact potential difference (LCPD), a quantity closely related to the distribution of charge on a surface [8–12]. Here we use a combination of STM, AFM, and KPFM to investigate naphthalocyanine, a single-molecule hydrogen-tautomerisation switch [13]. In particular, we show for the first time LCPD maps with submolecular resolution, and demonstrate that they reflect the intramolecular distribution of charge, as verified by comparison with density functional theory (DFT) calculations. We anticipate that our findings will lead to fundamental insights into single-molecule switching and bond formation—processes that are usually accompanied by an intra- or intermolecular redistribution of charge [14–16].

When a scanning probe tip is electrically connected to a conductive sample, a contact potential difference (CPD) will arise due to the different work functions of the tip and the sample. With KPFM, an offspring of AFM, local variations of this CPD can be measured [17]. This is done by applying a voltage between the sample and the oscillating AFM tip such that the electric field caused by the CPD and the resulting force on the tip are compensated as much as possible. The compensating voltage V^* for a certain tip position represents the LCPD signal and can be determined either with a feedback loop or by measuring the frequency shift (Δf) versus voltage (V) dependence [18]. In the latter case, V^* is defined by the position of the maximum of the resulting $\Delta f(V)$ parabola. With KPFM, the LCPD was measured for a wide range of surfaces, in some cases even with atomic resolution [19–22]. Moreover, KPFM was used to study the different charge states of single metal atoms [10], atomic point defects [11], and molecules [12] on thin insulating films. These studies suggest the possibility of measuring the charge distribution within single molecular adsorbates or nanostructures. However, the exact imaging mechanism of atomic-resolution KPFM is still under discussion [20, 23], and no submolecularly resolved KPFM images have so far been presented.

To demonstrate unambiguously that we can measure LCPD maps with submolecular resolution, we chose to investigate naphthalocyanine on two-monolayer-thick NaCl on Cu(111) [NaCl(2ML)/Cu(111)] at low temperature ($T = 5\,\mathrm{K}$). This system constitutes a molecular switch based on the STM-induced movement of the two inner hydrogen atoms in the free-base naphthalocyanine molecule [13]. It has several advantages for our study: The insulating NaCl film efficiently decouples the adsorbed molecules from the underlying metal, which prevents a strong hybridisation with the substrate electron states and facilitates the comparison of our results with calculations done for the free naphthalocyanine molecule. Furthermore, by comparing images of the different tautomers (which correspond to different adsorption orientations of the molecule), we can rule out that the contrast in the LCPD images is disturbed by a possible asymmetry of the microscope tip. The molecule maintains a flat adsorption geometry in both states, and the tautomerisation switching involves only a minor structural change. This excludes spurious geometrical effects on the LCPD measured that can be expected for systems in which the switching of a molecule is accompanied by a major change in the molecular structure [12].

In Fig. 1a, a constant-current STM image of a naphthalocyanine molecule on NaCl(2ML)/

Cu(111) is shown, recorded at a sample bias voltage of $V = 0.25\,\mathrm{V}$. The molecule appears as a cross-like structure, with a central protrusion surrounded by four lobes. There is no apparent asymmetry between the lobes parallel (H-lobes) and those perpendicular (N-lobes) to the two inner hydrogen atoms. This changes when the bias voltage is increased to $V = 0.6\,\mathrm{V}$ (Fig. 1b). This voltage corresponds to the lowest unoccupied molecular orbital (LUMO) resonance, and an image resembling the orbital of the free molecule is obtained [24]. The LUMO of naphthalocyanine has a two-fold symmmetry, with a nodal plane along the N-lobes. This enables the unambiguous determination of the tautomerisation state (i.e., the positions of the inner hydrogen atoms) from STM images recorded either with metal-terminated tips [13] or, as shown in Fig. 1b, with CO-terminated tips [25]. The CO-terminated tip had been prepared by picking up a single CO molecule, to increase the resolution in AFM imaging [5, 26]. After switching to AFM mode we recorded images of the same molecule (Fig. 1c.d). The images were acquired at two different tip–sample distances and exhibit clear atomic resolution of the C_6 rings in all four lobes. For the closer distance (Fig. 1c), the molecule appeared four-fold symmetric. When we increased the tip–sample distance, however, the symmetry was reduced to two-fold, and a distinct asymmetry developed in the centre region of the molecule, with brighter protrusions at the hydrogen-free N sites (Fig. 1d, see also Supplementary Information). This behaviour is reproduced in DFT-calculated maps of the CO–naphthalocyanine interaction energy (see Supplementary Information), as well as in the calculated electron density of the free naphthalocyanine molecule shown in Fig. 1e,f. This indicates that the atomic-scale contrast in the AFM images is mainly determined by the electron density at a certain height above the molecule. To further expose the asymmetry in the electron density, the difference between the two configurations, $A_\rho = [\rho_{0^\circ}(x,y) - \rho_{90^\circ}(x,y)]/\max(\rho)$, is shown in Fig. 1g,h, for different distances from the molecular (xy) plane. Here, ρ_{0° denotes the calculated electron density for the configuration overlaid in Fig. 1g,h, and ρ_{90° that for the tautomerised configuration (corresponding to a 90° rotation of the molecule). A_ρ is normalized with respect to the maximum value of the electron density, to give a better impression of the relative magnitude of the asymmetry, expressed in percent. Close to the molecular plane (Fig. 1g), the asymmetry is most pronounced in close vicinity of the positions of the inner hydrogen atoms. When moving away from the molecular plane (Fig. 1h), a much more extended asymmetry is observed, with higher electron density values above the N-lobes, even several bonds away from the centre of the molecule. The asymmetry in the charge distribu-

tion in the molecule yields a total quadrupole moment (including the charges of electrons and nuclei) of the molecule of $0.14\,e\mathrm{nm}^2$, where e is the elementary charge. In a point-charge model, this would correspond to pairs of positive (H-lobes) and negative (N-lobes) charges of $\pm 0.1\,e$ located 0.5 nm from the centre of the molecule. The calculated charge asymmetry between the different lobes is not reproduced in the AFM images in Fig. 1c,d, but we will show that it clearly manifests itself in images of the LCPD. The nonvanishing quadrupole moment together with the possibility of interchanging the positions of the donor-like H-lobes and the acceptor-like N-lobes by tautomerisation switching makes this molecule an ideal system for demonstrating KPFM contrast related to the intramolecular charge distribution.

For our KPFM measurements, we used the method illustrated in Fig. 2a: The AFM tip was moved consecutively to the intersections of a lateral grid above the molecule. At each point, a $\Delta f(V)$ spectrum was recorded (inset, red circles), and the position of the maximum of the fitted parabola (inset, solid black line) yielded the LCPD value, V^*, as well as the frequency shift at compensated LCPD, Δf^*, for that point. To demonstrate the possibility of KPFM with submolecular resolution, we first present measurements acquired with a metal-terminated tip obtained by indenting the tip into the bare Cu substrate. The LCPD images shown in Fig. 2b,c were recorded before and after switching the tautomerisation state of the imaged naphthalocyanine molecule. We observe a striking asymmetry between the H-lobes and the N-lobes, with larger values of V^* above the N-lobes. As expected, the tautomerisation switching had the effect of a 90° rotation of the LCPD image of the molecule, which excludes that the observed asymmetry between the H-lobes and the N-lobes is due to an asymmetric tip. The asymmetry is even more clearly visible in the difference image (Fig. 2d) obtained by subtracting the LCPD images of the initial and the switched configuration. The larger LCPD measured above the N-lobes would be expected for a charge asymmetry as in Fig. 1h: the more negatively charged N-lobes should lead to an increase in V^* [10]. However, the charge density in Fig. 1h contains only the electrons in a certain plane above the molecule. A more appropriate quantity to compare with our LCPD measurements is the electric field generated by the distribution of the total charge within the molecule, including all electrons and nuclei. The normalized asymmetry of the calculated electric field, $A_E = [E_{0^\circ}(x,y) - E_{90^\circ}(x,y)]/\max(E)$ is shown in Fig. 2e, at a distance $d = 0.5\,\mathrm{nm}$ above the molecular plane. Here, E_{0° and E_{90° denote the z-component of the electric fields, which we obtained by differentiating the DFT-calculated electrostatic potential for the initial

and the switched configuration, respectively. The asymmetry of the field generated by the quadrupole-like distribution of charge within the molecule exhibits a remarkable similarity with the difference image in Fig. 2d. This leads us to the conclusion that the submolecular resolution in the LCPD images reflects the total charge distribution within the molecule (a justification for the distances used for comparing the calculated electric fields to the experimental LCPD images can be found in the Supplemental Information).

Functionalizing a scanning probe tip with a single CO molecule is known to lead to enhanced resolution both in STM and AFM images [5, 26, 27]. However, the combination of KPFM and controlled tip functionalization has not been demonstrated until now. We have found that the CO-terminated tip also enables KPFM imaging with dramatically enhanced resolution compared to imaging with metal tips. The contrast in the CO-tip images of the LCPD was found to strongly depend on the height at which they were recorded, as shown in Fig. 3a-h. At distances further away from the molecule (Fig. 3a,b), the LCPD images recorded with the CO tip resemble those recorded with the Cu tip. However, as the tip–sample distance was decreased, gradually a more pronounced intramolecular contrast evolved (Fig. 3c-h). In Fig. 3i, a high-resolution LCPD image for the closest tip–sample distance investigated is shown. Pronounced features with larger values of V^* are observed above the outermost C_6 rings and in the vicinity of the four outer N atoms, as well as a distinct asymmetry between the C_5 rings in the H-lobes and the N-lobes. These features are absent from the simultaneously recorded Δf^* and current images (see Supplementary Information), which confirms that the LCPD signal is independent of these other channels. We attribute the different appearance of the lower left lobe and the upper right lobe in Fig. 3i to an asymmetry of the AFM tip or a slope in the background LCPD of the substrate, because in another measurement, such a feature was not found to switch with the tautomerisation state of the molecule (see Supplementary Information). Apart from that, the features in the LCPD image are well reproduced in the calculated electric field distribution in a plane above the free naphthalocyanine molecule (Fig. 3j). This further supports our interpretation that the submolecular resolution of our LCPD images reflects the distribution of charge within the molecule. The picture underlying this interpretation is in fact very intuitive: When the naphthalocyanine molecule is placed between the tip and the substrate, a locally varying contribution to the electric field arises due to the inhomogeneous charge distribution within the molecule. Compensating the total electric field during the KPFM measurement then results

in a variation of V^* that reflects the intramolecular charge distribution (longer-ranging contributions to the electrostatic interaction between tip and sample will only give an additional background that does not vary on the submolecular scale). Additional effects that could be imagined to affect the KPFM contrast include possible relaxations of the tip or the probed molecule, the finite polarizability of the tip, and the polarization of the probed molecule under application of an electric field [20] or due to chemical interactions [21]. However, we have found that the measured KPFM signal appears to be completely independent of the current and frequency shift signals (a bending of the tip molecule, e.g., should also affect the tunneling current). Together with the fact that the calculated electric field is already sufficient for a good qualitative description of our images, this leads us to the conclusion that the distribution of charge within the probed molecule and the electric field generated thereby is primarily responsible for the observed submolecular KPFM contrast.

We have imaged a single naphthalocyanine molecule with STM, AFM, and KPFM. While STM is sensitive only to the electron states close to the Fermi energy (the frontier orbitals of the molecule), we have shown that AFM and KPFM yield complementary images, which reflect either the total (energy-integrated) electron density (AFM) or the electric field generated by the total charge distribution (KFPM) within the molecule. Our finding opens up the possibility of directly imaging the charge distribution within single-molecule charge-transfer complexes, which hold promise for future applications such as solar photoconversion or energy storage [28, 29]. Furthermore, in combination with atomic manipulation techniques, it will now be possible to investigate, at the single-molecule level, how charge is redistributed when individual chemical bonds are formed between atoms and molecules on surfaces.

METHODS SUMMARY

Sample and tip preparation. A Cu(111) single crystal was cleaned by repeated sputtering and annealing cycles. Sodium chloride was evaporated at a sample temperature of $\sim 270\,\mathrm{K}$, leading to the formation of (100)-terminated NaCl islands having a thickness of mostly two atomic layers. Low coverages of naphthalocyanine and CO molecules ($\sim 0.1\,\%$ of a monolayer) were prepared *in situ* at a sample temperature of $\sim 10\,\mathrm{K}$. Well-defined tips terminated with Cu and CO were prepared by indenting the tip into the bare Cu surface and by picking up single CO molecules, respectively [5, 27].

STM, AFM, and KPFM measurements. All measurements were performed at a temperature of 5 K, with a homebuilt combined STM/AFM system based on the qPlus tuning fork design. The AFM and KPFM images were recorded in noncontact mode, with oscillation amplitudes between 35 and 45 pm. For the KPFM measurements, which lasted up to 33 h, we used a drift-correction procedure based on the recording of an STM reference image [30]. Within the voltage range used to determine V^* and Δf^* from the fitted $\Delta f(V)$ curves, we did not observe any deviations from the parabolic shape, apart from the normal noise level. In all our measurements, we used STM orbital imaging to determine the tautomerisation state of the molecule.

DFT calculations. The calculations were performed for the free naphthalocyanine molecule using the highly optimized plane-wave code CPMD [V3.15, Copyright IBM Corp. 1990-2011, Copyright MPI für Festkörperforschung Stuttgart 1997-2001]. The Perdew-Burke-Ernzerhof exchange-correlation functional and *ab initio* norm-conserving pseudopotentials were used. In the pseudopotential method, the valence electrons are accurately described outside a certain core region ($\sim 0.06\,\mathrm{nm}$ for carbon atoms), whereas the core electrons are eliminated within the frozen-core approximation. This approximation yields an excellent description of the total electron density at the distances in Fig. 1. The size of the unit cell was $3.2 \times 3.2 \times 1.6\,\mathrm{nm}^3$. The structural optimization was performed until the forces on all atoms were below $10^{-3}\,\mathrm{eV/nm}$, and a cutoff energy of 2 keV was used for a single k point (Γ).

REFERENCES

* fmo@zurich.ibm.com

[1] Piva, P. G. *et al.* Field regulation of single-molecule conductivity by a charged surface atom. *Nature* **435**, 658 (2005).

[2] Sugimoto, Y. *et al.* Chemical identification of individual surface atoms by atomic force microscopy. *Nature* **446**, 64 (2007).

[3] Ashino, M. *et al.* Atomically resolved mechanical response of individual metallofullerene molecules confined inside carbon nanotubes. *Nature Nanotech.* **3**, 337 (2008).

[4] Albers, B. J. *et al.* Three-dimensional imaging of short-range chemical forces with picometre resolution. *Nature Nanotech.* **4**, 307 (2009).

[5] Gross, L., Mohn, F., Moll, N., Liljeroth, P. & Meyer, G. The chemical structure of a molecule resolved by atomic force microscopy. *Science* **325**, 1110 (2009).

[6] Vitali, L. *et al.* Portrait of the portential barrier at metal-organic nanocontacts. *Nature Mater.* **9**, 320 (2010).

[7] Swart, I., Sonnleitner, T. & Repp, J. Charge state control of molecules reveals modification of the tunneling barrier with intramolecular contrast. *Nano Lett.* **11**, 1580 (2011).

[8] Sommerhalter, C., Matthes, T. W., Glatzel, T., Jäger-Waldau, A. & Lux-Steiner, M. C. High-sensitivity quantitative Kelvin probe microscopy by noncontact ultra-high-vacuum atomic force microscopy. *Appl. Phys. Lett.* **75**, 286 (1999).

[9] Barth, C. & Henry, C. R. Surface double layer on (001) surfaces of alkali halide crystals: A scanning force microscopy study. *Phys. Rev. Lett.* **98**, 136804 (2007).

[10] Gross, L. *et al.* Measuring the charge state of an adatom with noncontact atomic force microscopy. *Science* **324**, 1428 (2009).

[11] König, T. *et al.* Measuring the charge state of point defects on MgO/Ag(001). *J. Am. Chem. Soc.* **131**, 17544 (2009).

[12] Leoni, T. *et al.* Controlling the charge state of a single redox molecular switch. *Phys. Rev. Lett.* **106**, 216103 (2011).

[13] Liljeroth, P., Repp, J. & Meyer, G. Current-induced hydrogen tautomerization and conductance switching of naphthalocyanine molecules. *Science* **317**, 1203 (2007).

[14] Grill, L. *et al.* Nano-architectures by covalent assembly of molecular building blocks. *Nature Nanotech.* **2**, 687 (2007).

[15] Wang, W. *et al.* Manipulating localized molecular orbitals by single-atom contacts. *Phys. Rev. Lett.* **105**, 126801 (2010).

[16] Mohn, F. *et al.* Reversible bond formation in a gold-atom–organic-molecule complex as a molecular switch. *Phys. Rev. Lett.* **105**, 266102 (2010).

[17] Nonnenmacher, M., O'Boyle, M. P. & Wickramasinghe, H. K. Kelvin probe force microscopy. *Appl. Phys. Lett.* **58**, 2921 (1991).

[18] Burke, S. A. *et al.* Determination of the local contact potential difference of PTCDA on NaCl: a comparison of techniques. *Nanotechnology* **20**, 264012 (2009).

[19] Enevoldsen, G. H., Glatzel, T., Christensen, M. C., Lauritsen, J. V. & Besenbacher, F. Atomic scale Kelvin probe force microscopy studies of the surface potential variations on the TiO_2(110) surface. *Phys. Rev. Lett.* **100**, 236104 (2008).

[20] Bocquet, F., Nony, L., Loppacher, C. & Glatzel, T. Analytical approach to the local contact potential difference on (001) ionic surfaces: Implications for Kelvin probe force microscopy. *Phys. Rev. B* **78**, 035410 (2008).

[21] Sadewasser, S. *et al.* New insights on atomic-resolution frequency-modulation Kelvin-probe force-microscopy imaging of semiconductors. *Phys. Rev. Lett.* **103**, 266103 (2009).

[22] Kawai, S., Glatzel, T., Hug, H.-J. & Meyer, E. Atomic contact potential variations of Si(111)-7×7 analyzed by Kelvin probe force microscopy. *Nanotechnology* **21**, 245704 (2010).

[23] Masago, A., Tsukada, M. & Shimizu, M. Simulation method of Kelvin probe force microscopy at nanometer range and its application. *Phys. Rev. B* **82**, 195433 (2010).

[24] Repp, J., Meyer, G., Stojkovic, S. M., Gourdon, A. & Joachim, C. Molecules on insulating films: scanning-tunneling microscopy imaging of individual molecular orbitals. *Phys. Rev. Lett.* **94**, 026803 (2005).

[25] Gross, L. *et al.* High-resolution molecular orbital imaging using a *p*-wave STM tip. *Phys. Rev. Lett.* **107**, 086101 (2011).

[26] Gross, L. *et al.* Organic structure determination using atomic-resolution scanning probe microscopy. *Nature Chem.* **2**, 821 (2010).

[27] Bartels, L., Meyer, G. & Rieder, K.-H. Controlled vertical manipulation of single CO molecules with the scanning tunneling microscope: A route to chemical contrast. *Appl. Phys. Lett.* **71**, 213 (1997).

[28] Jäckel, F. *et al.* Investigating molecular charge transfer complexes with a low temperature scanning tunneling microscope. *Phys. Rev. Lett.* **100**, 126102 (2008).

[29] Tao, C. *et al.* Spatial resolution of a type II heterojunction in a single bipolar molecule. *Nano Lett.* **9**, 3963 (2009).

[30] Mohn, F., Gross, L. & Meyer, G. Measuring the short-range force field above a single molecule with atomic resolution. *Appl. Phys. Lett.* **99**, 053106 (2011).

Supplementary Information is linked to the online version of the paper at www.nature.com/nature.

Acknowledgements We would like to thank Jascha Repp, Rolf Allenspach, and Walter Riess for helpful comments. Financial support from the EU projects Herodot and ARTIST is gratefully acknowledged.

Author contributions F.M., L.G., and G.M. performed the experiments. F.M. and N.M. did the DFT calculations. F.M. wrote the manuscript. All authors discussed the results and commented on the manuscript.

The authors declare no competing financial interests. Correspondence and requests for materials should be addressed to F.M. (fmo@zurich.ibm.com).

Mohn_fig1

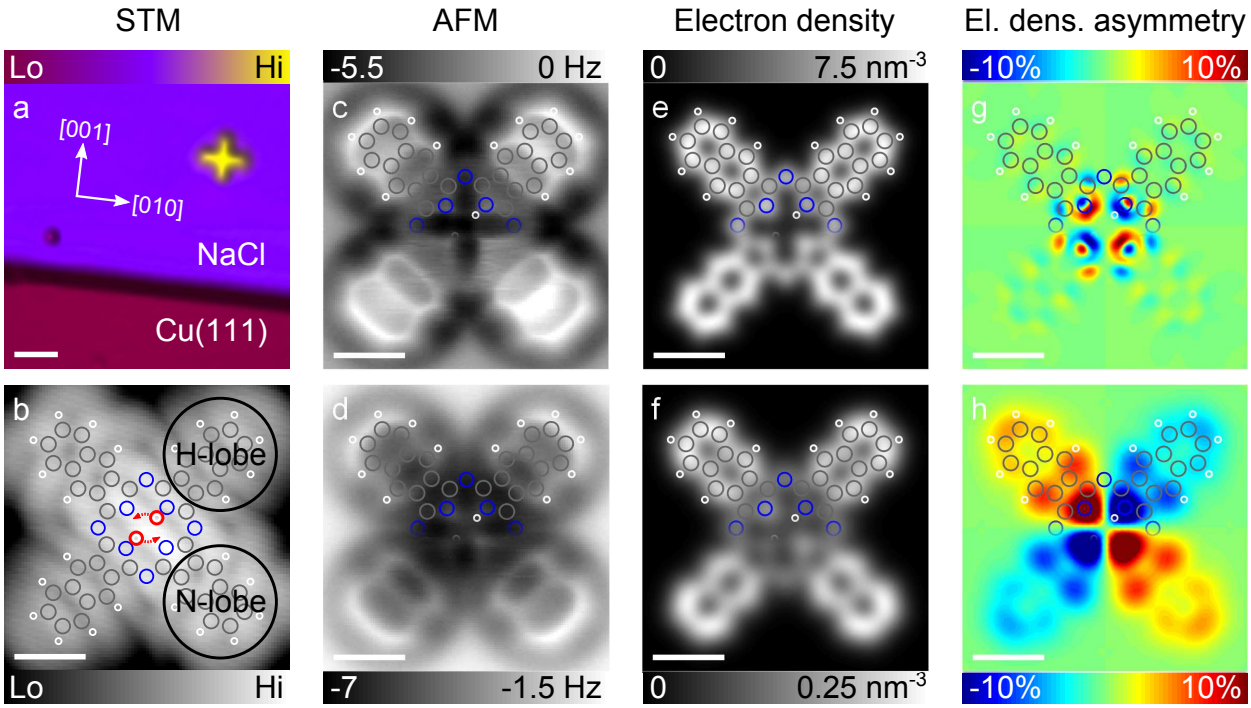

FIG. 1. STM and AFM imaging of naphthalocyanine on NaCl(2ML)/Cu(111). **a**, STM constant-current image ($I = 2\,\mathrm{pA}$, $V = 0.25\,\mathrm{V}$) recorded at the edge of a two-monolayer NaCl island on Cu(111). A single naphthalocyanine molecule (yellow) and a single CO molecule (depression close to the NaCl step edge) can be identified. The crystallographic directions of the topmost NaCl layer are indicated. **b**, STM constant-current image of a naphthalocyanine molecule ($I = 2\,\mathrm{pA}$, $V = 0.6\,\mathrm{V}$). The image was recorded with a CO-terminated tip. The positions of the central hydrogens and the tautomerisation path are highlighted in red, and the definition of H-lobes and N-lobes is illustrated. **c**,**d** Constant-height AFM frequency-shift images of the same molecule as in **b** measured with a CO-terminated tip. The images were recorded at distances $z = 0.145\,\mathrm{nm}$ (**c**), and $z = 0.175\,\mathrm{nm}$ (**d**) above the height determined by the STM set point ($I = 2\,\mathrm{pA}$, $V = 0.2\,\mathrm{V}$) over the substrate. **e**,**f** Cuts through the DFT-calculated electron density of a naphthalocyanine molecule at distances $d = 0.2\,\mathrm{nm}$ (**e**) and $d = 0.3\,\mathrm{nm}$ (**f**) from the molecular plane. **g**,**h** The asymmetry of the calculated electron density at $d = 0.1\,\mathrm{nm}$ (**g**) and $d = 0.4\,\mathrm{nm}$ (**h**) from the molecular plane. The scale bars are 2 nm in **a** and 0.5 nm in all other panels, and the DFT-calculated atomic positions are overlaid in **b** and in the upper halves of **c**-**h**. Carbon, hydrogen, and nitrogen atoms are coloured in gray, white, and blue, respectively.

Mohn_fig2

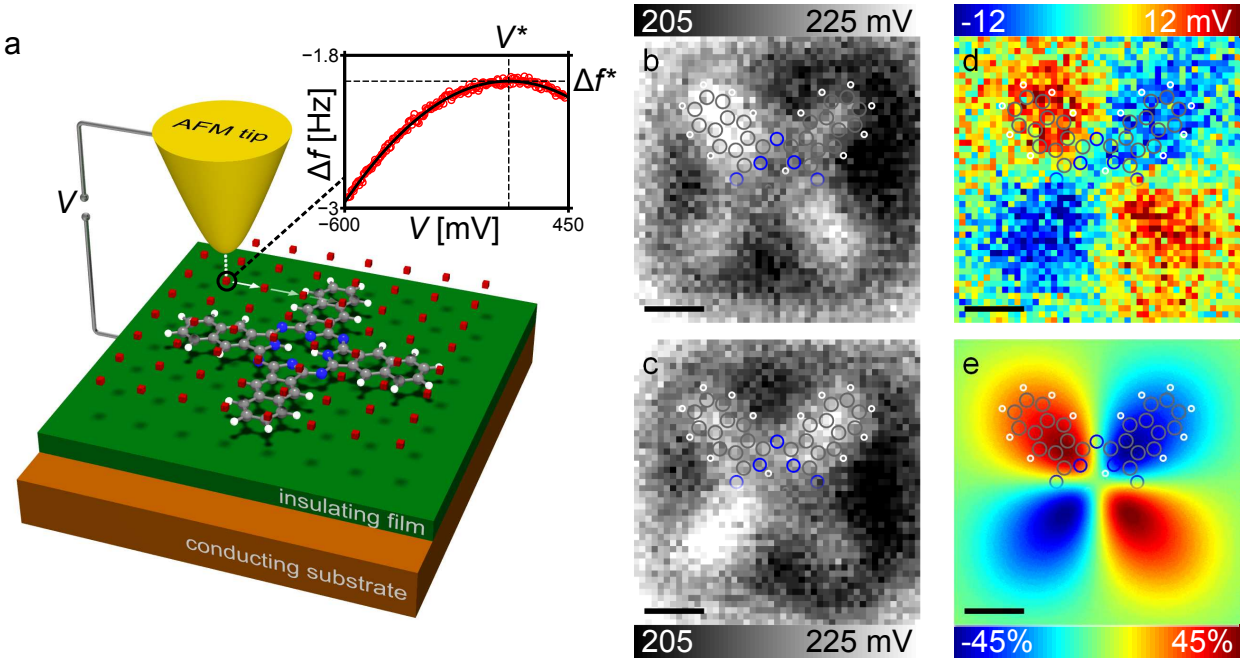

FIG. 2. LCPD images of the tautomerisation switching of naphthalocyanine. **a**, Schematic of the measurement principle. At each tip position, the frequency shift is recorded as a function of the sample bias voltage (inset, red circles). The maximum of the fitted parabola (inset, solid black line) yields V^* and Δf^* for that position. **b**,**c**, LCPD images of naphthalocyanine on NaCl(2ML)/Cu(111) before (**b**) and after (**c**) switching the tautomerisation state of the molecule. The images were recorded with a Cu-terminated tip on a 64×64 lateral grid at constant height [$z = 0.1\,\mathrm{nm}$ above the height determined by the STM set point ($I = 3\,\mathrm{pA}$, $V = 0.2\,\mathrm{V}$) over the substrate]. **d**, Difference image obtained by subtracting image **c** from **b**. **e**, DFT-calculated asymmetry of the z-component of the electric field above a free naphthalocyanine molecule at a distance $d = 0.5\,\mathrm{nm}$ from the molecular plane. All scale bars are 0.5 nm, and the DFT-calculated atomic positions are overlaid in the upper halves of **b**-**e**. Carbon, hydrogen, and nitrogen atoms are coloured in gray, white, and blue, respectively.

Mohn_fig3

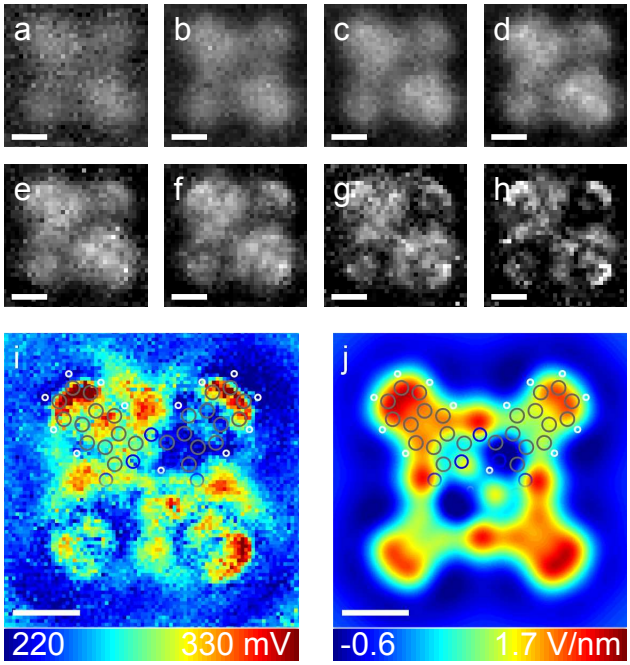

FIG. 3. Enhanced resolution in LCPD images by tip functionalization with CO. **a**-**h**, LCPD images of naphthalocyanine on NaCl(2ML)/Cu(111) measured with a CO-terminated tip. The images were recorded on a 40×40 lateral grid at constant height, for different distances that decrease from **a** to **h** [$z = 0.29$, 0.27, 0.25, 0.23, 0.22, 0.21, 0.20, and 0.19 nm above the height determined by the STM set point ($I = 2$ pA, $V = 0.2$ V) over the substrate]. The colour scale ranges from 240 mV (black) to 340 mV (white). **i**, LCPD image recorded with the same tip and imaging parameters as in **h**, but on a 92×92 lateral grid. **j**, DFT-calculated z-component of the electric field above a free naphthalocyanine molecule at a distance $d = 0.3$ nm from the molecular plane. All scale bars are 0.5 nm, and the DFT-calculated atomic positions are overlaid in the upper halves of **i** and **j**. Carbon, hydrogen, and nitrogen atoms are coloured in gray, white, and blue, respectively.